THE ASTROPHYSICAL JOURNAL, 301:98–104, 1986 February 1

NGC 1320: A FEEBLE, HIGH-IONIZATION SEYFERT 2 GALAXY[1]

M. M. DE ROBERTIS AND D. E. OSTERBROCK
Lick Observatory, Board of Studies in Astronomy and Astrophysics, University of California, Santa Cruz
Received 1985 June 17; accepted 1985 August 5

ABSTRACT

Emission-line strengths and widths are reported for NGC 1320, a Seyfert 2 galaxy that is unusual in having both a quite high ionization spectrum, as well as rather narrow lines and a relatively weak featureless continuum. The narrow-line region is evidently quite small in this galaxy, and the observed gas has not been accelerated to velocities as high as the velocities observed in most other Seyfert galaxies.

Subject headings: galaxies: individual — galaxies: internal motions — galaxies: Seyfert

I. INTRODUCTION

High-ionization emission lines (including He II, and possibly [Fe VII] and [Fe X]) from the nucleus of a spiral galaxy are part of the definition of a Seyfert-type spectrum (e.g., see Weedman 1977). Another part of the spectral definition requires that the emission lines be "broad"—taken usually to mean narrow-line widths in excess of 300 km s^{-1} (e.g., Shuder and Osterbrock 1981; De Robertis and Osterbrock 1985). Thus it is quite uncommon, if not contradictory, to find a high-ionization Seyfert 2 spectrum with narrow-line full widths at half-maximum (FWHM) less than 300 km s^{-1}.

Mark 1388, discussed by Osterbrock (1985), has an unusual high-ionization, narrow-line Seyfert 2 galaxy with a strong featureless continuum. Osterbrock and Pogge (1985) also analyzed a sample of narrow-line Seyfert 1 galaxies, which differ from Mrk 1388 in that each shows evidence for a broad-line region, although with a relatively low velocity dispersion.

We present the data for NGC 1320 (= Mark 607 = MCG − 1-9-36), a second high-ionization, narrow-line Seyfert galaxy, but with a very weak featureless continuum and correspondingly low luminosity.

II. OBSERVATIONS

In their objective-prism discovery paper, Markarian and Lipovetsky (1974) remarked that NGC 1320 is an edge-on spiral galaxy and might "form a pair" with NGC 1321 (= Mrk 608), a nearby spheroidal object. W. C. Keel drew our attention to NGC 1320 as a potential Seyfert galaxy with a nearby companion galaxy. We observed it and present measurements of NGC 1320 taken from five spectral scans taken with the Shane 3 m telescope at Lick Observatory. Two of them are high-dispersion scans taken with the image dissector scanner (IDS) (Robinson and Wampler 1972; Miller, Robinson, and Wampler 1976; Miller, Robinson, and Schmidt 1980). The remaining three scans were taken with the transmission CCD spectrograph, using 420 and 600 line mm^{-1} grisms for low and moderate resolution and a 150 line mm^{-1} echelle grism ("echism") in the fifth and sixth orders (cross-dispersed by a 300 line mm^{-1} grism) for high resolution. The slit width was 0.54 mm, projecting to 2″.1 on the sky. The detector was a TI 800 × 800 CCD (Lauer *et al.* 1984). The estimated seeing profile (FWHM) for the 420 line mm^{-1} spectrum (on which the relative flux measurements described below depend almost completely) was ∼4″, while for the 600 line mm^{-1} spectrum it was 1″.5. Both exposures were taken within 50 minutes of the meridian—that is, with zenith angles less than 44°. The relevant observational details are summarized in Table 1. We also obtained one spectrum of NGC 1321 with the CCD spectrograph, using the 420 line mm^{-1} grism.

The IDS reduction procedure is described in Osterbrock (1981). The CCD data were reduced in the following manner: pixel-to-pixel variations were removed by dividing each image by an appropriate (quartz lamp) flat field. The relevant spectral rows in each image were co-added and sky-subtracted to produce the raw spectrum. These spectra were reduced to wavelength units using exposures on standard comparison lamps taken at the beginning of the night for the local dispersion, and sky lines recorded simultaneously with the galaxy spectra for the zero points. The counts were transformed to energy units per unit wavelength, per unit area, per unit time, using standard stars taken at the beginning and ending of the night. For most of the spectra, broad atmospheric absorption in the atmospheric A and B bands was eliminated by dividing the spectra by these same standard stars. All of the two-dimensional analysis was carried out using the VISTA

[1] *Lick Observatory Bulletin*, No. 1020.

TABLE 1

SUMMARY OF OBSERVATIONS

Date	Time (minutes)	Resolution (Å)	Instrument	Wavelength (Å)
1984 Dec 30/31	20	12	CCD 420 lines mm^{-1}	4000–8000
1984 Dec 30/31	50	3.5	CCD 150 lines mm^{-1}	5700–6800
1985 Jan 20/21	30	6	CCD 600 lines mm^{-1}	5800–7900
1985 Feb 17/18	64	5	IDS 1200 lines mm^{-1}	4200–5450
1985 Feb 17/18	64	5	IDS 1200 lines mm^{-1}	5900–7150

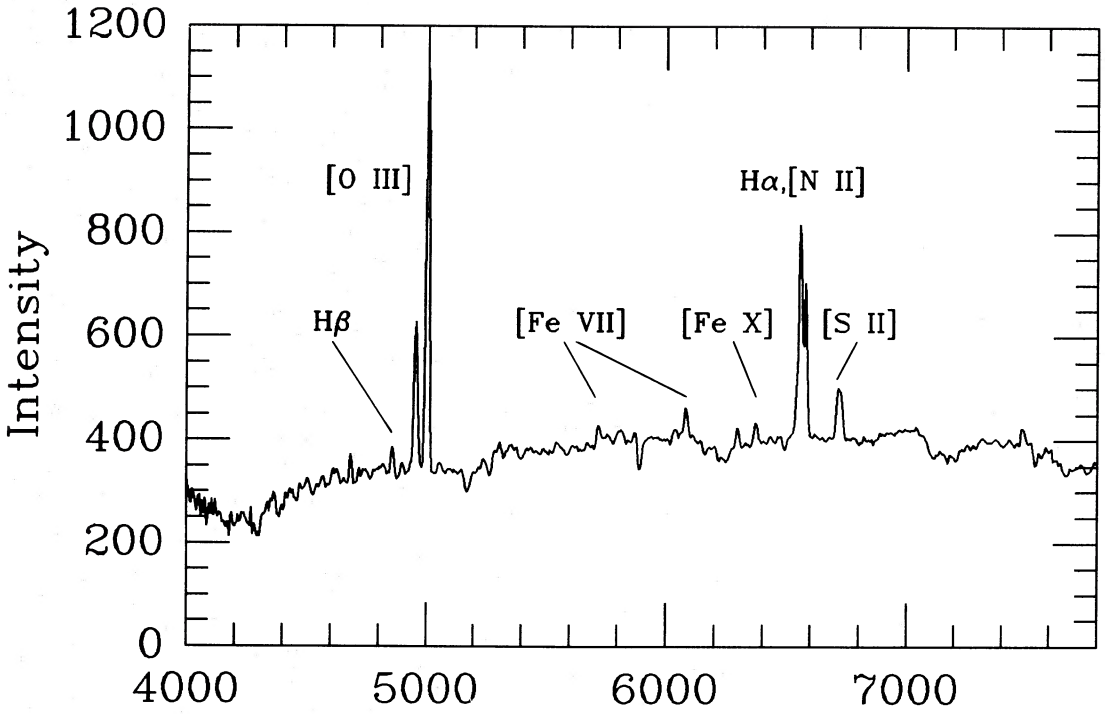

FIG. 1.—Observed spectral scan of NGC 1320, 4000–7800 Å, plotted as relative flux in energy units per unit wavelength interval vs. wavelength in rest system of emitting object.

program (Terndrup, Lauer, and Stover 1984) on the Lick Observatory VAX 11/780.

Figure 1 shows a low-resolution tracing of the spectrum of NGC 1320 covering the range 4200–7800 Å. It is immediately apparent that it contains high-ionization emission lines of He II λ4686, [Fe VII] λλ5721, 6087, and [Fe X] λ6375, *and* a substantial stellar continuum dominated by an old stellar population, as shown by the G band and prominent Mg I, Ca I, and TiO absorption features.

As noted by Markarian and Lipovetsky (1974), NGC 1320 is an edge-on spiral. Assuming that the face-on cross section of the galaxy is circular, the axial ratio 0.32 estimated from the Palomar Observatory Sky Survey plates implies that the stellar disk is inclined by over 70° to the line of sight. The heliocentric redshift measured from the high-resolution echism spectrum is 0.0094 ± 0.0001, which, for a Hubble constant of 50 km s^{-1} Mpc^{-1}, puts NGC 1320 at a distance of 56 Mpc.

The spheroidal galaxy NGC 1321 lies 94″ north of NGC 1320 at a projected linear separation of 26 kpc. The spectrum of NGC 1321 is a composite early K III type without emission lines, typical of an old stellar population. Its heliocentric redshift, based only on the Balmer absorption lines, is 0.0092 ± 0.0003. The line-of-sight velocity difference between these galaxies is thus 60 ± 100 km s^{-1}. Unless the relative velocity component in the plane of the sky is substantially larger than this, these galaxies probably constitute a bound system. (There is no evidence from the Palomar Observatory Sky Survey for any asymmetries that might have resulted from a significant tidal interaction.) There is a G-type star with zero redshift 6″.5 east of the center of NGC 1321, as shown by our long-slit spectrum. This star and the nucleus of NGC 1321 are the "central pair of starlike objects" mentioned by Markarian and Lipovetsky (1974).

To estimate correctly weak-line fluxes and widths, and the strength of the featureless continuum in a spectrum of this sort, the stellar continuum must be properly subtracted. NGC 1321 proved to be an ideal template, since not only does it have an early K III spectral type which is most commonly used as a model for removing an old population integrated stellar absorption-line spectrum, but also it was observed under nearly identical conditions to NGC 1320. The optical continua have similar apparent brightnesses. To carry out a more quantitative analysis, the continuum of NGC 1321 was normalized to that of NGC 1320 in the wavelength range 5400–5500 Å where there are no apparent emission or absorption features in either spectrum. We then subtracted an arbitrary fraction of NGC 1321's spectrum ("stellar continuum") from NGC 1320's (using spectra taken with the same grism at the same resolution) and judged the results by eye. With an assumed ratio of 90% stellar continuum to 10% featureless continuum at 5400 Å, the G band disappeared, and the Mg I and TiO features were almost removed. For smaller ratios, the absorption features remained rather prominent, while for larger ratios, spurious "emission features" were introduced into the spectrum of NGC 1320. (Na I λ5893 absorption could not be removed from the spectrum of NGC 1320 with any reasonable ratio. This line can arise in the interstellar medium of an underlying galaxy as well as in the stars' atmospheres. It is not surprising then to find a large difference in the equivalent widths of this feature, since NGC 1320 is an edge-on spiral galaxy and NGC 1321 an elliptical galaxy.) We have adopted as the best fit a featureless continuum fraction of $f_C = 0.10 \pm 0.05$.

Figure 2 presents the "best-fit" stellar continuum-subtracted spectrum (i.e., the featureless continuum plus emission lines remain) for NGC 1320. We emphasize that to produce this spectrum we simply subtracted a scaled spectrum of NGC 1321 from NGC 1320 to isolate this underlying featureless continuum. It is likely, however, that there are small

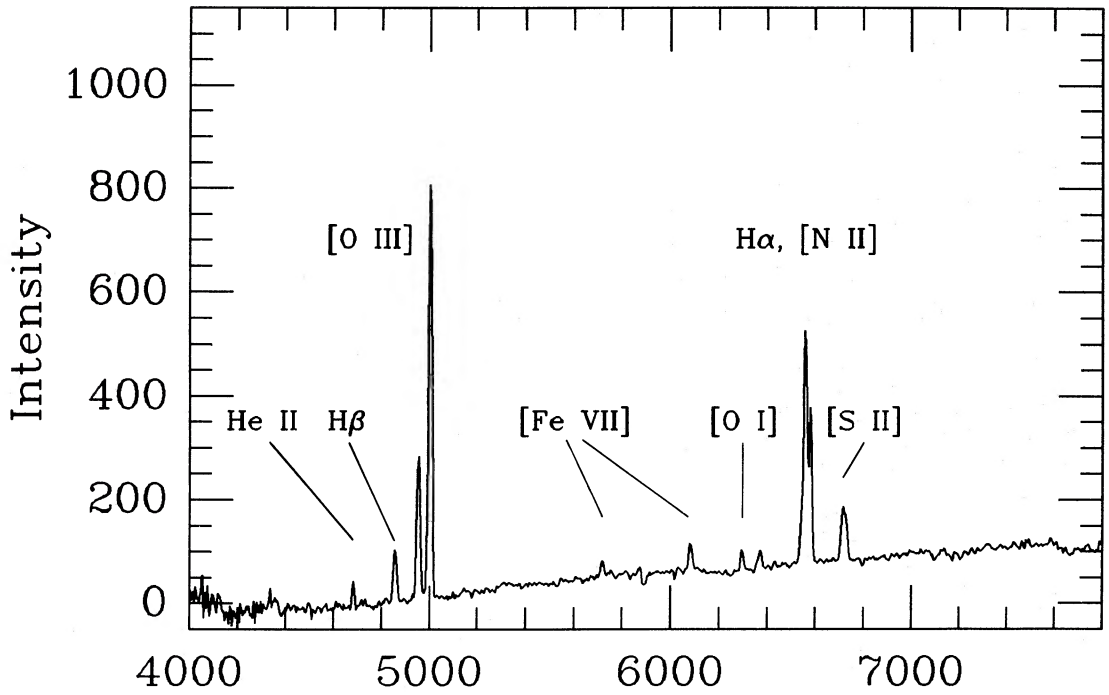

FIG. 2.—Spectral scan of NGC 1320, 4000–7800 Å, with integrated stellar absorption-line spectrum subtracted. Coordinates as in Fig. 1.

color differences between the stellar continua of the two galaxies. For this reason, there are likely to be small errors in the shape of the featureless continuum shown in Figure 2. In fact, relative intensities ≤ 0 in Figure 2 reveal a small color difference between the integrated populations in the sense that NGC 1321 appears to be slightly bluer than NGC 1320. In any event, it is apparent that this featureless continuum is very red. In fact, over the very small baseline of 2500 Å, it has an optical spectral index (before correction for reddening), defined by $f_\nu \propto \nu^{-\alpha}$, of $\alpha \approx 6.5 \pm 1$. This result is not sensitive to the degree of stellar continuum subtracted, or apparently to the template adopted. W. C. Keel kindly provided us with a synthesis (Keel 1982) of the spectrum of NGC 3384 (at a similar resolution to NGC 1320) which, while redder than NGC 1321, is still representative of an old stellar population. The results of the subtraction procedure were not altered significantly using this template, except that perhaps the spectral index α decreased to a value $5.0 < \alpha < 6.5$.

III. MEASUREMENTS

a) Line Strengths

Table 2 contains the relevant information on the relative emission-line strengths in NGC 1320. These measurements were made primarily from the 420 line mm^{-1} scan with the underlying stellar continuum removed, using NGC 1321 as a template as outlined in § II. (Only the relative intensities of Hβ and He II λ4686 changed significantly from measurements made on the original unsubtracted spectrum.) The higher dispersion scans, especially the 600 line mm^{-1} scan, were used to check and improve the line ratios derived in this way. There was good agreement between the ratios measured on the high- and low-dispersion scans. The Hα, [N II] λλ6548, 6583 blend was measured as a single emission feature in the low-dispersion scan, and the appropriate line ratios were determined from the fifth-order echism spectrum. The [Fe X] λ6375 intensity was estimated by measuring the entire [O I] λ6364, [Fe X] λ6375 blend and subtracting 0.3 times the intensity measured for [O I] λ6300. Columns (1) and (2) give the ion and wavelength for each line measured. Columns (3) and (4) give the observed and reddening-corrected fluxes relative to Hβ. Because these observations were taken with a slit width of 2″.1, the absolute fluxes are not determined to high accuracy. The relative fluxes, however, are known to much better accuracy. The calculated differential refraction between He II λ4686, the shortest wavelength line measured, and λ6000, the effective wavelength of the television guidance system, was always <0″.4—small compared with the seeing diameter and slit width.

TABLE 2

RELATIVE EMISSION-LINE FLUXES

Ion (1)	Wavelength (Å) (2)	$F/F(H\beta)$ Observed[a] (3)	$I/I(H\beta)$ Corrected[b] (4)	Equivalent Width (Å) (5)
H I	4340	0.21	0.26	...
[O III]	4363	0.29	0.35	...
He II	4686	0.43	0.46	...
H I	4861	1.00	1.00	32
[O III]	4959	3.57	3.45	90
[O III]	5007	9.86	9.37	242
[Fe VII]	5721	0.29	0.22	4
He I	5876	0.17	0.13	2
[Fe VII]	6087	0.57	0.40	7
[O I]	6300	0.38	0.26	4
[Fe X]	6375	0.34	0.22	4
H I	6563	4.86	3.10	55
[N II]	6583	3.36	2.13	38
[S II]	6716	0.93	0.58	10
[S II]	6731	1.07	0.66	11

[a] $F(H\beta)_{obs} = 1.4 \times 10^{-14}$ ergs cm^{-2} s^{-1}.
[b] $I(H\beta)_{cor} = 6.1 \times 10^{-14}$ ergs cm^{-2} s^{-1}, $E_{B-V} = 0.43$.

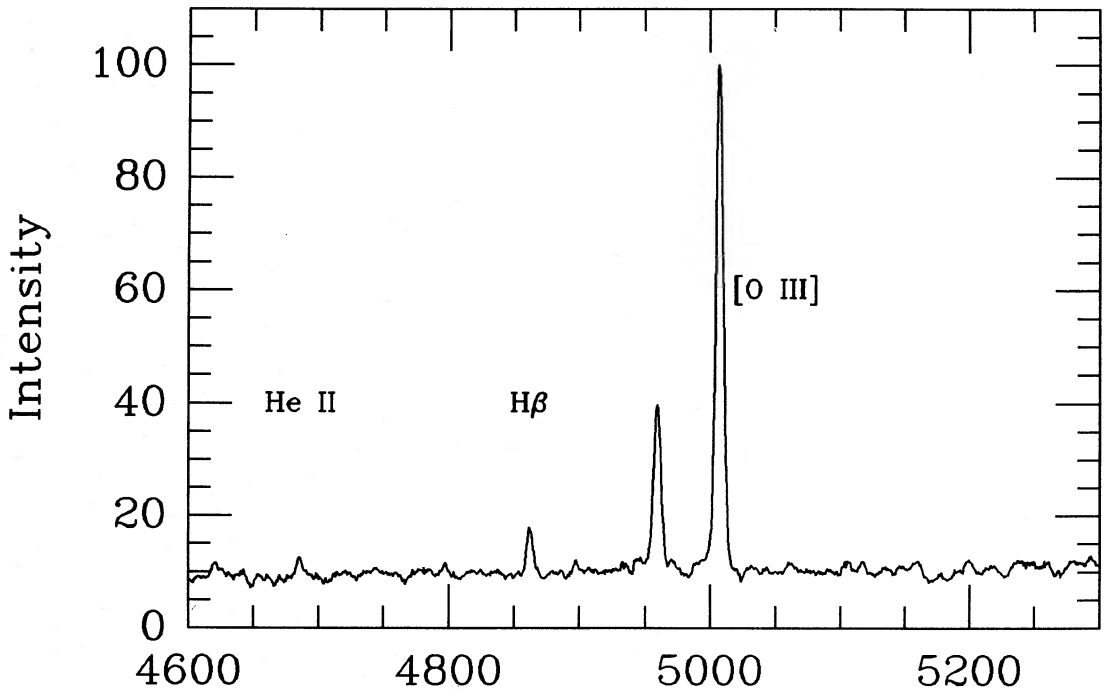

FIG. 3.—High-dispersion spectral scan of NGC 1320, 4600–5300 Å. Coordinates as in Fig. 1.

The adopted reddening corrections are based on the Whitford interstellar reddening curve, as fitted by Miller and Mathews (1972), assuming an intrinsic Hα/Hβ ratio of 3.1 (Ferland and Netzer 1983; Halpern and Steiner 1983; Gaskell and Ferland 1984). The observed ratio $H\alpha/H\beta = 4.9 \pm 0.7$ corresponds to $E(B-V) = 0.43 \pm 0.12$ mag. This in turn leads to an extinction $A_V = 1.4 \pm 0.4$ mag. The observed Hβ flux of 1.4×10^{-14} ergs s^{-1} cm^{-2}, corrected for this extinction, becomes 6.1×10^{-14} ergs s^{-1} cm^{-2}. Column (5) gives the relevant equivalent widths relative to the featureless continuum at the position of each emission line. Because the featureless continuum is most uncertain in the blue according to our subtraction procedure, we do not list the equivalent widths for lines in which the continuum intensity is ≤ 0 (see § II). The results for He I λ5876, which is very weak and affected by Na I absorption, are uncertain by a factor of 2, while the uncertainties for the remaining lines range from a few to perhaps 30%.

b) *Line Widths*

Figures 3 and 4 display the high-dispersion spectra from which the line widths were primarily measured. Figure 3 is the IDS blue scan, while Figure 4 show the fifth order of the CCD echism spectrum. Neither spectrum has had the stellar continuum subtracted. We followed the procedure for calculating line widths described in Osterbrock and Pogge (1985) and De Robertis and Osterbrock (1985). That is, the observed FWHM was assumed to be the quadrature sum of the intrinsic and instrumental FWHMs. Emission-line profiles from the comparison-lamp spectra of Cd I, Hg I, Ne I, and He I were assumed to represent the instrumental profile. The resulting intrinsic FWHMs, except for Hβ and [O I] λ6300, are essentially those listed in Table 3.

The FWHM of Hβ measured in this way was 220 km s^{-1}, while the Hα FWHM was 310 km s^{-1}. As Figure 3 shows, Hβ is a relatively weak emission line, and its profile is substantially affected by the Hβ absorption from the underlying galaxy spectrum. The Hα profile is much affected, since it is a stronger emission line, and a weaker absorption line in the integrated stellar spectrum.

To eliminate these blending effects from the emission-line profiles as completely as possible, we used continuum-subtracted versions of the high-dispersion scans for the final measurements. The low-resolution scan of NGC 1321 again was used as the template spectrum, since we had no high-dispersion scan of an absorption-line galaxy taken with the same instrumental setup. A four-point Lagrangian interpolation scheme was used to artificially reduce the sampling to match that in the high-dispersion spectra. This procedure is not as accurate as using a high-dispersion template scan, but is better than making no correction. The continuum-subtracted scan of the 4600–5300 Å region differs only slightly from the unsubtracted scan of the same region in Figure 3. The main

TABLE 3

LINE WIDTHS

Ion	Wavelength (Å)	FWHM (km s^{-1})
He II	4686	200:
H I	4861	275
[O III]	4959	290
[O III]	5007	265
[Fe VII]	5721	425
He I	5876	385:
[Fe VII]	6087	455
[O I]	6300	185
[Fe X]	6375	395
H I	6563	320
[N II]	6583	300
[S II]	6716	260
[S II]	6731	250

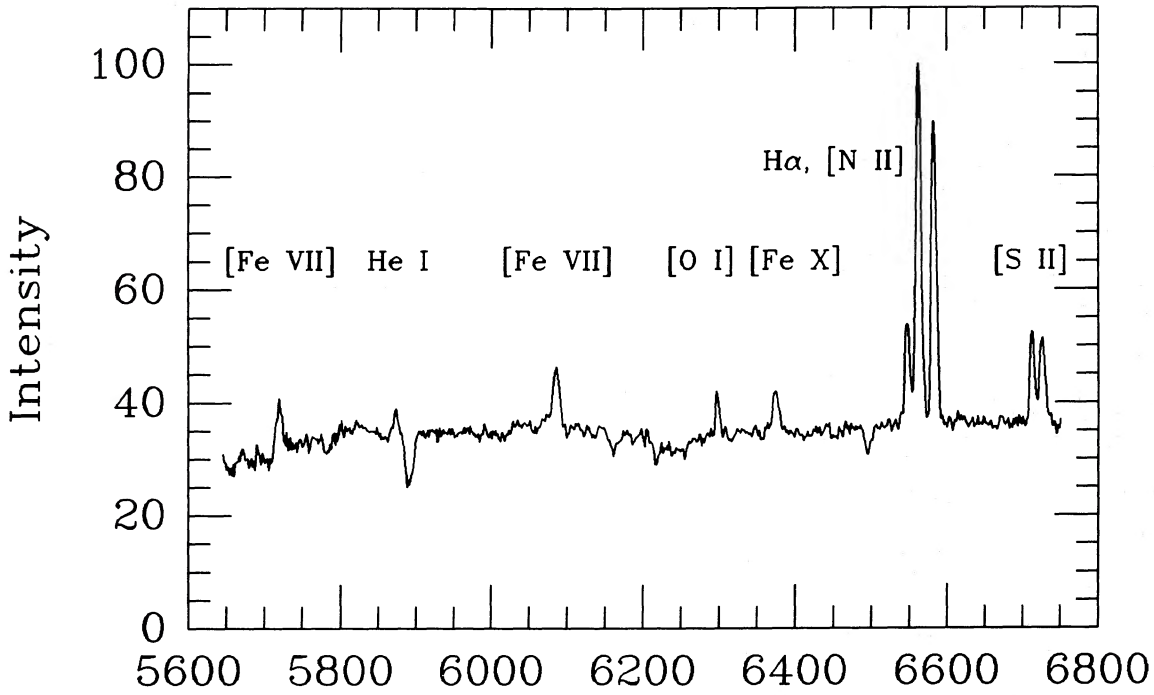

FIG. 4.—High-dispersion spectral scan of NGC 1320, 5600–6800 Å. Coordinates as in Fig. 1.

difference is in the relative amplitudes of Hβ and He II λ4686, with respect to the nearby [O III] λλ4959, 5007.

The final FWHMs, measured from the corrected scans, are listed in Table 3. Note that the FWHMs of Hβ and Hα are now in much better agreement. Besides Hβ, the only FWHM to change more than a few percent was [O I] λ6300, which was measured as 170 km s^{-1} in the uncorrected scan. The uncertainty in the final FWHMs is ~10% for most of the profiles. In the high-dispersion scans, Hγ and [O III] λ4363 were too weak to provide useful FWHMs. We listed the measured FWHM for He II λ4686, but the small width given is probably in error as a result of this line's weakness in the high-dispersion scans. The quoted width was derived using the best estimated profile from our spectrum.

Note that the line widths in Table 3 are very narrow for a Seyfert 2 spectrum. In fact, apart from the high-ionization lines, they are more representative of observed absorption-line widths in galaxies (see below). The [O I] λ6300 profile is the narrowest, and the high-ionization [Fe VII] λλ5721, 6087 and [Fe X] λ6375 profiles are the broadest.

c) *Continuum*

Corrected for reddening, the total continuum flux for NGC 1320 at 5000 Å is $1.5 \times 10^{-14} \pm 0.3$ ergs s^{-1} cm^{-2} $Å^{-1}$, the contribution of the featureless continuum being ~15%. Table 4 gives the monochromatic, reddening-corrected, featureless continuum luminosity at 4861 Å (in ergs $s^{-1}Å^{-1}$) for a sample of Seyfert 2 galaxies and LINERs taken from Koski (1978) and Costero and Osterbrock (1977), and NGC 1320. Errors in the logarithm of the luminosity are ±0.3. We have adopted the classification of LINERs given by Ferland and Netzer (1983) and have eliminated Mrk 378 and Mrk 507, which Shuder and Osterbrock (1981) showed are not Seyfert 2 galaxies from Koski's (1978) list. While NGC 1320 is definitely not a LINER, it lies at the low-luminosity end of the active galaxtic nucleus phenomenon comprised of Seyfert galaxies and LINERs. The absolute magnitude for the featureless continuum alone is $M_{\lambda 5000} = -17.5$, and $M_{\lambda 5000} = -20.0$ for the stellar plus featureless continuum, together within the aperture 2″.1 × 7″.0. Clearly, the nonthermal source is not intrinsically luminous. The blue apparent magnitude for the entire galaxy estimated by Vorontsov-Velyaminov and Arkipova (1964) and by Markarian and Lipovetsky (1974) is 14. This corresponds to an absolute blue magnitude $M_B = -20$, which is close to the most probable value for Seyfert 2 galaxies found by Meurs and Wilson (1984).

If we apply the same reddening correction to the featureless continuum derived from the emission lines, then the reddening-corrected spectral index is related to the observed spectral index by $\alpha_{cor} = \alpha - 2$; or $\alpha_{cor} > 3.5$. Even though the baseline for this estimate is small, there is no doubt but the the continuum corrected for extinction in this way is red and steep in the optical region. According to Koski (1978), the featureless con-

TABLE 4

CONTINUUM LUMINOSITIES

Galaxy	Type	log $L_{\lambda 4861}$
Mrk 1	Seyfert 2	39.3
Mrk 3	Seyfert 2	39.6
Mrk 34	Seyfert 2	40.1
Mrk 176	Seyfert 2	40.3
Mrk 198	Seyfert 2	39.5
Mrk 268	Seyfert 2	39.9
Mrk 270	Seyfert 2	38.0
Mrk 273	Seyfert 2	41.0
Mrk 348	Seyfert 2	38.9
Mrk 573	Seyfert 2	38.8
NGC 6764	LINER	39.7
Mrk 298	LINER	39.6
Mrk 700	LINER	39.9
3C 178	LINER	39.5
PKS 2322−12	LINER	40.0
Mrk 607	Seyfert 2	38.9

tinuum source suffers less reddening than the emission-line gas in most Seyfert 2 galaxies, which would argue that we have overestimated the continuum luminosity and the spectral index is even steeper than given above. Recent reddening models considered by De Zotti and Gaskell (1985) for Seyfert 1 galaxies however, if applied to Seyfert 2 galaxies, suggest that the featureless continuum may be more heavily reddened than the emission-line gas. In this event, the featureless continuum luminosity has been underestimated, and the spectral index is flatter than noted. If [Fe x] λ6375 is a result of photoionization as inferred in other Seyfert galaxies (Osterbrock 1981; Penston *et al.* 1984), then the ionizing continuum must clearly extend well past 234 eV. The UV and soft X-ray continua must be significantly flatter than the extrapolated optical continuum, since the observed equivalent width of Hβ requires $\alpha \leq 1.5$ (Searle and Sargent 1968). Even so, to maintain the high degree of ionization observed, the emission-line region must be considerably smaller than in more "normal" Seyfert 2 galaxies. If this reasoning is correct, one might hope to detect narrow-line profile variability on time scales of perhaps months or years.

NGC 1320 has been detected at 12, 25, 60, and 100 μm by *IRAS* (Lonsdale *et al.* 1985). According to the criteria of de Grijp *et al.* (1985), NGC 1320 is a "warm galaxy" with a 25–60 μm spectral index of 0.88 and a 12–60 μm spectral index of 1.20. Apparently then, between 0.8 and 12 μm, the nonthermal continuum must flatten considerably. "Warm galaxies" have relatively large infrared luminosities. It has been suggested that the excess infrared emission comes from dust which absorbs and reradiates energy from high-frequency continuum photons (e.g., Rieke 1978; Carter 1984). It is not known how extended this dust distribution might be, but it is possible that the dust responsible for the infrared emission is also responsible for the reddening inferred from the optical emission-line ratios.

IV. ANALYSIS

NGC 1320 has very narrow emission-line profiles. All but the highest ionization lines have FWHMs less than the canonical 300 km s^{-1} mentioned in the definition of a Seyfert galaxy. Phillips, Charles, and Baldwin (1983) and Whittle (1985*a*, *b*) have found that some relatively low-luminosity Seyfert 2 galaxies have narrower lines (down to FWHM $\approx$ 200 km s^{-1}), but few, if any, of these objects have [Fe VII] and [Fe X] as strong as in NGC 1320.

The mean line widths measured in NGC 1320 are more characteristic of disk rotation velocities (Whitmore, Rubin, and Ford 1984), or of the upper end of dispersion velocities in the distribution of galactic bulges (Kormendy and Illingworth 1982). It is possible then that the emission-line gas in this particular narrow-line region is in equilibrium with the underlying gravitational potential, especially since the galaxy is viewed almost edge-on. Certainly the gas in the narrow-line region has not been accelerated to as high velocities as in the emission-line regions in most other Seyfert galaxies. Yet the ionization in NGC 1320 is very high.

While the profile widths are narrow, there is a trend, in the sense that the low-ionization emission lines, [O I] λ6300 and [S II] $\lambda\lambda$6716, 6731, are narrowest and the high-ionization lines, [Fe VII] λ5721, 6087 and [Fe X] λ6375, are the broadest. Thus, there is a better line width–ionization potential correlation in NGC 1320 than a line width–critical density correlation. (Unfortunately, [O III] λ4363, an important diagnostic in determining critical density correlations, is too weak to measure on our high-dispersion scan.) Although Seyfert 2 galaxies tend to have better critical density–FWHM correlations, De Robertis and Osterbrock (1985) have shown that some Seyfert 2 galaxies do have correlations of line width with ionization potential. We also note that even at the highest resolution, all the narrow lines appear to be symmetric.

TABLE 5

TEMPERATURE AND DENSITY ESTIMATES

T (10^4 K)	N_e (10^5 cm^{-3})
O^{2+} Region	
1.0.....	6.8
1.5.....	0.9
1.7.....	$\sim$0
S^+ Region	
0.5.....	5.0
1.0.....	6.6
1.5.....	7.5

We can calculate the mean electron temperature T and density N_e in the O^{2+} and S^+ regions from the reddening-corrected ratios of $I(\lambda4959 + \lambda5007)/I(\lambda4363) = 52$, and $I(\lambda6716)/I(\lambda6731) = 0.9$, respectively. These results are contained in Table 5.

V. CONCLUSIONS

NGC 1320 is a high-ionization, edge-on Seyfert 2 galaxy with a weak, featureless continuum and very narrow emission lines. Narrow lines with FWHMs < 300 km s^{-1} are not usually associated with the Seyfert phenomenon, and high-ionization lines are not usually correlated with such a weak, nonstellar continuum. The tendency for the lowest ionization profiles to be narrowest does fit the line width–ionization potential correlation found in some Seyfert galaxies.

The fraction of featureless continuum estimated from the optical spectrum is $\sim$0.1. The featureless continuum is very red, with an optical spectral index less than 3.5 if the continuum is corrected for reddening derived from the emission-line ratios. In order to account for the observed high-ionization emission lines, this continuum must flatten drastically in the ultraviolet. Even so, the high ionization combined with the low luminosity of the featureless continuum requires that the characteristic size of the narrow-line region is considerably less than in most other observed and analyzed Seyfert galaxies. NGC 1320 is also a "warm galaxy," with a relatively large infrared luminosity. The galaxy itself has an absolute magnitude close to the most probable value for the Seyfert 2 luminosity function of Meurs and Wilson (1984). While it is not possible to provide a quantitative estimate for the number of Seyfert galaxies like NGC 1320 that might exist, objective-prism surveys are not sensitive to a population with a weak continuum and narrow emission lines, and there may be many more than we now know.

We are indebted to W. C. Keel for directing our attention to NGC 1320 and for many helpful discussions concerning the subtraction of the stellar continuum. We would like to thank W. G. Mathews for useful discussions and R. W. Goodrich for making his programs available for the density and temperature calculations. We are also grateful to the National Science Foundation for partial support of this research under grant AST 83-11585. Finally, we would like to thank the referee for useful suggestions.

REFERENCES

Carter, D. 1984, *Astr. Express*, **1**, 61.
Costero, R., and Osterbrock, D. E. 1977, *Ap. J.*, **211**, 675.
de Grijp, M. H. K., Miley, G. K., Lub, J., and de Jong, T. 1985, *Nature*, **314**, 240.
De Robertis, M. M., and Osterbrock, D. E. 1985, *Ap. J.*, **301**, in press.
De Zotti, G., and Gaskell, C. M. 1985, *Astr. Ap.*, **147**, 1.
Ferland, G. J., and Netzer, H. 1983, *Ap. J.*, **264**, 105.
Gaskell, C. M., and Ferland, G. J. 1984, *Pub. A.S.P.*, **96**, 393.
Halpern, J. P., and Steiner, J. E. 1983, *Ap. J. (Letters)*, **269**, L37.
Keel, W. C. 1982, Ph.D. thesis, University of California, Santa Cruz.
Kormendy, J., and Illingworth, G. 1982, *Ap. J.*, **256**, 460.
Koski, A. T. 1978, *Ap. J.*, **223**, 56.
Lauer, T. R., Miller, J. S., Osborne, C. S., Robinson, L. B., and Stover, R. J. 1984, *SPIE Proc.*, **445**, 132.
Lonsdale, C. J., Helou, G., Good, J. C., and Rice, W. 1985, *Cataloged Galaxies and Quasars Observed in the IRAS Survey*, (Pasadena: Jet Propulsion Laboratory).
Markarian, B. E., and Lipovetsky, V. A. 1974, *Astrofizika*, **10**, 307 (English transl. in *Astrophysics*, **10**, 185 [1974]).
Meurs, E. J. A., and Wilson, A. S. 1984, *Astr. Ap.*, **136**, 206.
Miller, J. S., and Mathews, W. G. 1972, *Ap. J.*, **172**, 593.
Miller, J. S., Robinson, L. B., and Schmidt, G. D. 1980, *Pub. A.S.P.*, **92**, 702.
Miller, J. S., Robinson, L. B., and Wampler, E. J. 1976, *Adv. Electronics Electron Phys.*, **40B**, 693.
Osterbrock, D. E. 1981, *Ap. J.*, **246**, 696.
———. 1985, *Pub. A.S.P.*, **97**, 587.
Osterbrock, D. E., and Pogge, R. W. 1985, *Ap. J.*, **297**, 166.
Penston, M. V., Fosbury, R. A. E., Boksenberg, A., Ward, M. J., and Wilson, A. S. 1984, *M.N.R.A.S.*, **208**, 347.
Phillips, M. M., Charles, P. A., and Baldwin, J. A. 1983, *Ap. J.*, **266**, 485.
Rieke, G. 1978, *Ap. J.*, **226**, 550.
Robinson, L. B., and Wampler, E. J. 1972, *Pub. A.S.P.*, **84**, 161.
Searle, L., and Sargent, W. L. W. 1968, *Ap. J.*, **153**, 1005.
Shuder, J. M., and Osterbrock, D. E. 1981, *Ap. J.*, **250**, 55.
Terndrup, D., Lauer, T. R., and Stover, R. J. 1984, *Lick Obs. Tech. Rep.*, No. 33.
Vorontsov-Velyaminov, I. A., and Arkipova, B. P. 1964, *Morphological Catalog of Galaxies* (Moscow: University of Moscow).
Weedman, D. W. 1977, *Ann. Rev. Astr. Ap.*, **15**, 69.
Whitmore, B. C., Rubin, V. C., and Ford, W. K., Jr. 1984, *Ap. J.*, **287**, 66.
Whittle, M. 1985*a*, *M.N.R.A.S.*, **213**, 1.
———. 1985*b*, *M.N.R.A.S.*, **213**, 33.

M. M. De Robertis and D. E. Osterbrock: Lick Observatory, Board of Studies in Astronomy and Astrophysics, University of California, Santa Cruz, CA 95064